JOURNAL OF THERMOPHYSICS AND HEAT TRANSFER
Vol. 22, No. 1, January–March 2008

Discontinuous Spectral Element Approach for Solving Transient Radiative Transfer Equations

J. M. Zhao* and L. H. Liu†
Harbin Institute of Technology, 150001 Harbin, People's Republic of China

DOI: 10.2514/1.32688

A discontinuous spectral element method is presented to solve transient radiative heat transfer in multidimensional semitransparent media. The transient term is discretized by the Crank–Nicolson scheme, and the spatial discretization is conducted using the discontinuous spectral element approach. The salient features of the discontinuous spectral element method are that it possesses high-order accuracy, has properties such as local conservation, and its solutions are allowed to be discontinuous across interelement boundaries. The inherent discontinuity acceptable property of the discontinuous spectral element method allows efficient and accurate capturing of the sharp wave front of the transient radiative transfer process. A special treatment for the problem with diffuse irradiation at the boundary is presented to mitigate the ray effect encountered in solving the transient radiative transfer equation. The performance of the discontinuous spectral element method is verified by three test cases. The predicted results by the discontinuous spectral element method agree well with reported benchmark solutions in the references.

Nomenclature

c	=	speed of light, m/s
f	=	adjustment parameter for temporal discretization
G	=	incident radiation, W/m^2
I	=	radiative intensity, $W/(m^2sr)$
I_b	=	blackbody radiative intensity, $W/(m^2sr)$
K	=	kth element
L	=	width of slab, side length, m
L_R	=	reference scale, m
M	=	number of discrete ordinate directions
$\mathbf{n}_{\partial K}$	=	unit outward normal vector of the boundary of the element
N_{el}	=	total number of elements
N_{sk}	=	number of solution nodes on the element
N_t	=	number of discretized time steps
N_θ	=	number of angular discretization for 1-D cases
N_θ^{c}	=	number of equivalent collimated beams
p	=	order of polynomial expansion
$\mathbf{q}$	=	heat flux vector
q_c	=	heat flux of collimated irradiation at direction $\mathbf{\Omega}_c$, W/m^2
$\mathbf{r}$	=	spatial coordinates vector
S	=	source term function
$\tilde{S}$	=	modified source term in the temporal discretized equation
s	=	Lagrange ray coordinates
T	=	temperature, K
t	=	time, s
t^*	=	dimensionless time
β	=	extinction coefficient $\beta = (\kappa_a + \kappa_s)$, m^{-1}
$\tilde{\beta}$	=	modified extinction coefficient in the temporal discretized equation
δ	=	Dirac delta function
ε_w	=	wall emissivity
κ_a	=	absorption coefficient, m^{-1}
κ_s	=	scattering coefficient, m^{-1}
σ	=	Stefan–Boltzmann constant, $W/(m^2K^4)$
τ_L	=	optical thickness, $\tau_L = \beta L$
Φ	=	scattering-phase function
ϕ	=	nodal basis function
$\mathbf{\Omega}$	=	unit vector of the radiation direction
Ω	=	solid angle
ω	=	single scattering albedo

Subscripts

B	=	direct component
c	=	collimated component
d	=	diffuse component in collimated irradiation
i, j	=	spatial node index
n	=	time-step index
S	=	diffuse component in diffuse irradiation
w	=	value at the wall

Superscripts

c	=	collimated
m	=	mth discrete ordinate direction

I. Introduction

IN RECENT years, with the development of some new technologies such as short-pulse laser processing of materials [1–3], light-tissue interaction [4–8], and optical imaging [9–12], which often require good understanding of the transient process of radiation transfer, transient radiative transfer in participant media has attracted the interest of many researchers. Because of the existence of transient terms, the transient radiative transfer equation (TRTE) explicitly has the property of hyperbolic type equation. Compared with the steady-state radiative transfer equation (RTE), the accurate solution of the TRTE is more difficult. Recently, methods for the solution of the transient radiative transfer can be mainly put into three classes: 1) probabilistic-based methods, such as the Monte Carlo method [13–16]; 2) methods based on integral formulation of the TRTE, such as the integral equation method (IE) [17–19]; and 3) methods based on the TRTE in differential form, such as the spherical harmonics method [20], discrete ordinates method (DOM) [21–24], finite volume method (FVM) [25,26], finite element method (FEM) [27], and discontinuous finite element method (DFEM) [28]. The Monte Carlo method has advantages such as clear physical meaning, good

Received 8 June 2007; revision received 12 August 2007; accepted for publication 15 August 2007.

*Ph.D. Candidate, School of Energy Science and Engineering, 92 West Dazhi Street; cxzjm@hit.edu.cn.

†Professor, School of Energy Science and Engineering, 92 West Dazhi Street; lhliu@hit.edu.cn (Corresponding Author).

adaptability, and reliability; however, it requires a large amount of computational effort for the solution of the transient problem. The IE method has good accuracy for the solution of the hyperbolic type differential equation, such as it can capture the discontinuous wave front accurately [17], but it is too complex to be adapted to the media with anisotropically scattering and relatively difficult to be implemented for the problem with complex geometry. The methods based on the differential form of the TRTE are efficient and easy to apply to the problems with complex media and boundary properties, among which the DOM and FVM have received considerable attention. One of the major drawbacks of the already developed DOM and FVM is that they present relatively large false scattering and the transient wave front cannot be captured efficiently and accurately. A similar problem exists in the FEM [27]. The development of a method that is stable, with higher-order accuracy and less false scattering, and that can accurately capture the sharp wave front is still the highlight and needs further contribution. Recently, based on the discontinuous Galerkin approach (DG), Liu and Hsu [28] developed and analyzed transient radiative transfer in graded index media by a DFEM. Their work initially demonstrated that methods based on the DG scheme have good adaptability for the solution of the transient radiative transfer problem.

The DG approach was first introduced to the community of radiative transfer by Cui and Li [29,30]; they developed a DFEM for solving the steady-state radiative transfer equation. The DG approach has many advantages compared with the conventional Galerkin method and has been successfully applied to the solution of many physics and engineering problems [31–34]. In the DG approach, the interelement continuity is released and the approximation space comprises discontinuous functions. This property is expected to be ideal for the solution of the transient radiative transfer problem, such as to accurately capture the sharp wave front. An introduction and comprehensive review of the DG approach are found in Cockburn et al. [35,36]. The spectral element method (SEM) [37] combines the competitive advantages of high-order accuracy of the spectral method and the flexibility of the finite element method. In SEM, the physical domain is broken up into several elements and within each element a spectral representation based on orthogonal polynomials (such as the Chebyshev polynomial and Legendre polynomial) is used. However, the traditional SEM are based on global continuous formulation, in which the functions of approximation space are not allowed to be discontinuous across elements and thus lack the salient features of DG-based methods. Recently, by combining both the advantages of the DG approach and spectral element approximation, Zhao and Liu [38] presented a discontinuous spectral element method (DSEM) for the solution of the steady-state radiative transfer problem. The DSEM is stable, of high-order accuracy, and shows better performance compared with its counterparts based on the continuous scheme, such as the Galerkin spectral element method (GSEM) and the least-squares spectral element method (LSSEM) [39].

By considering valuable properties of the DSEM [38] that promise the solution of the transient radiative transfer in this paper (such as elemental conservatism, high-order accuracy, and inherent elemental discontinuity acceptability) as an extension of the DSEM, a discontinuous spectral element approach for transient radiative transfer is developed. The performances of the DSEM for solving the TRTE are studied and verified. In the following section, the governing equations for transient radiative transfer are first presented. Then the discretization process of the governing equation by the DSEM is given. Finally, three test cases are given to verify the performances of the DSEM for solving the TRTE.

II. Governing Equations

A. Transient Radiative Transfer Equation

The TRTE in absorbing, emitting, and scattering media can be written as

$$\frac{\partial I(\mathbf{r},\mathbf{\Omega},t)}{c\partial t}+\mathbf{\Omega}\cdot\nabla I(\mathbf{r},\mathbf{\Omega},t)+\beta I(\mathbf{r},\mathbf{\Omega},t)=S(\mathbf{r},\mathbf{\Omega},t) \quad (1)$$

where the source function $S(\mathbf{r},\mathbf{\Omega},t)$ is defined as

$$S(\mathbf{r},\mathbf{\Omega},t)=\kappa_a I_b(\mathbf{r},\mathbf{\Omega},t)+\frac{\kappa_s}{4\pi}\int_{4\pi} I(\mathbf{r},\mathbf{\Omega}',t)\Phi(\mathbf{\Omega}',\mathbf{\Omega})\mathrm{d}\Omega' \quad (2)$$

The initial and the boundary conditions are needed for Eq. (1) to uniquely define a solution. The initial condition is given by

$$I(\mathbf{r},\mathbf{\Omega},0)=I_0(\mathbf{r},\mathbf{\Omega}) \quad (3)$$

and the boundary condition prescribed on the inflow boundary ($\mathbf{n}_w\cdot\mathbf{\Omega}<0$) is given as

$$\begin{aligned} I(\mathbf{r}_w,\mathbf{\Omega},t)&=\varepsilon_w I_{bw}(\mathbf{r}_w,t)\\ &+\frac{1-\varepsilon_w}{\pi}\int_{\mathbf{n}_w\cdot\mathbf{\Omega}'>0} I(\mathbf{r}_w,\mathbf{\Omega}',t)|\mathbf{n}_w\cdot\mathbf{\Omega}'|\mathrm{d}\Omega'\\ &+q_c(\mathbf{r}_w,t)\delta(\mathbf{\Omega}-\mathbf{\Omega}_c) \end{aligned} \quad (4)$$

where $q_c(\mathbf{r}_w,t)$ denotes the heat flux of collimated irradiation at direction $\mathbf{\Omega}_c$.

B. Treatment of Collimated Irradiation

For the collimated irradiation problem, radiative energy concentrates in one direction. As a result, the usually used angular quadrature schemes such as S_N approximation cannot be used effectively to do angular integration. The methods based on the discrete ordinate equation in Eq. (1) cannot work effectively, and special treatment for this kind of problem is thus necessary. The commonly taken approach [12,21] is to decompose the transient radiative intensity to a collimated component and a diffuse component by applying the superposition principle to Eq. (1), which is similar to the treatment of the steady-state collimated irradiation problem [40]. The radiative intensity is then decomposed as

$$I(\mathbf{r},\mathbf{\Omega},t)=I_c(\mathbf{r},\mathbf{\Omega},t)+I_d(\mathbf{r},\mathbf{\Omega},t) \quad (5)$$

where $I_c(\mathbf{r},\mathbf{\Omega},t)$ denotes the collimated component and $I_d(\mathbf{r},\mathbf{\Omega},t)$ denotes the diffuse component. The collimated component $I_c(\mathbf{r},\mathbf{\Omega},t)$ is governed by

$$\begin{aligned} &\frac{\partial I_c(\mathbf{r},\mathbf{\Omega},t)}{c\partial t}+\mathbf{\Omega}\cdot\nabla I_c(\mathbf{r},\mathbf{\Omega},t)+\beta I_c(\mathbf{r},\mathbf{\Omega},t)\\ &=\frac{\mathrm{d}I_c(s)}{\mathrm{d}s}+\beta I_c(s)=0 \end{aligned} \quad (6)$$

which can be solved analytically for its simple form. The solution can be written with Lagrange description as

$$I_c(s)=I_c(0)\exp\left(-\int_0^s\beta(s)\mathrm{d}s\right) \quad (7)$$

where $s=ct$ is the Lagrange coordinates along the ray trajectory, and its origin ($s=0$) is the place from which the photon is started. The diffuse component $I_d(\mathbf{r},\mathbf{\Omega},t)$ is governed by

$$\frac{\partial I_d(\mathbf{r},\mathbf{\Omega},t)}{c\partial t}+\mathbf{\Omega}\cdot\nabla I_d(\mathbf{r},\mathbf{\Omega},t)+\beta I_d(\mathbf{r},\mathbf{\Omega},t)=S^+(\mathbf{r},\mathbf{\Omega},t) \quad (8a)$$

with boundary condition

$$\begin{aligned} I_d(\mathbf{r}_w,\mathbf{\Omega},t)&=\varepsilon_w I_{bw}(\mathbf{r}_w,t)\\ &+\frac{1-\varepsilon_w}{\pi}\int_{\mathbf{n}_w\cdot\mathbf{\Omega}'>0} I(\mathbf{r}_w,\mathbf{\Omega}',t)|\mathbf{n}_w\cdot\mathbf{\Omega}'|\mathrm{d}\Omega' \end{aligned} \quad (8b)$$

where the modified source term $S^+(\mathbf{r},\mathbf{\Omega},t)$ is given by

$$S^+(\mathbf{r},\mathbf{\Omega},t)=\kappa_a I_b(\mathbf{r},\mathbf{\Omega},t)+\frac{\kappa_s}{4\pi}\left[\int_{4\pi} I_d(\mathbf{r},\mathbf{\Omega}',t)\Phi(\mathbf{\Omega}',\mathbf{\Omega})\mathrm{d}\Omega'+q_c(\mathbf{r},t)\Phi(\mathbf{\Omega}_c,\mathbf{\Omega})\right] \tag{9}$$

The transient incident radiation distribution function $G(\mathbf{r},t)$ and radiative heat flux distribution function $\mathbf{q}(\mathbf{r},t)$ can be calculated, respectively, as

$$G(\mathbf{r},t)=\int_{4\pi} I(\mathbf{r},\mathbf{\Omega},t)\mathrm{d}\Omega=\int_{4\pi} I_d(\mathbf{r},\mathbf{\Omega},t)\mathrm{d}\Omega+q_c(\mathbf{r},t) \tag{10a}$$

$$\mathbf{q}(\mathbf{r},t)=\int_{4\pi} I(\mathbf{r},\mathbf{\Omega},t)\mathbf{\Omega}\,\mathrm{d}\Omega=\int_{4\pi} I_d(\mathbf{r},\mathbf{\Omega},t)\mathbf{\Omega}\,\mathrm{d}\Omega+q_c(\mathbf{r},t)\mathbf{\Omega}_c \tag{10b}$$

C. Special Treatment for Diffuse Irradiation

As demonstrated in Sec. IV, the direct discretization of Eq. (1) with transient diffuse irradiation will encounter ray effect. The interpretation of this kind of ray effect is illustrated in Fig. 1. A transient diffuse irradiation is suddenly originating from the left wall, due to the emission or diffuse reflection of the wall. Consider a point P inside the media at a small instant t: only the radiation from a small strip on the left wall can reach P, which makes the transient energy confined to a very small solid angle $\Delta\Omega$ and makes the angular distribution of radiative intensity contain discontinuities, as shown in Fig. 1. In this case, the angular distribution of radiative intensity is difficult to be efficiently and accurately integrated by general angular discretization schemes such as S_N approximation. The inaccuracy in angular integration will then cause ray effect. This is similar to the steady-state case (namely, the "diffuse strip loading" case studied by Ramankutty and Crosbie [41]), which results in the ray effect when solving by the standard discrete ordinates method.

In this section, a special treatment is presented to mitigate the ray effect. Based on the idea that the transient directional radiative intensity at any given point inside the media is due to two sources (namely, photons directly originating from the boundary surface and photons being scattered or emitted inside the media), the radiative intensity can be decomposed into the direct and the diffuse components as

$$I(\mathbf{r},\mathbf{\Omega},t)=I_B(\mathbf{r},\mathbf{\Omega},t)+I_S(\mathbf{r},\mathbf{\Omega},t) \tag{11}$$

where $I_B(\mathbf{r},\mathbf{\Omega},t)$ accounts for the transient intensity component due to photons directly originating from the boundary surface, and $I_S(\mathbf{r},\mathbf{\Omega},t)$ accounts for the transient intensity component due to photons being scattered or emitted inside the media. It should be noted that this kind of approach was initially proposed in the solution of steady-state radiative transfer problems such as the modified differential approximation of Olfe [42] and Modest [43] and the modified discrete ordinates methods of Ramankutty and Crosbie [41], which successfully mitigate the ray effects in the standard discrete ordinates method.

As previously defined, the direct component $I_B(\mathbf{r},\mathbf{\Omega},t)$ is governed by

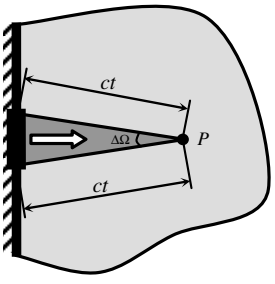

Fig. 1 Schematic interpretation of the ray effect in the solution of the transient radiative transfer problem.

$$\frac{\partial I_B(\mathbf{r},\mathbf{\Omega},t)}{c\partial t}+\Omega\cdot\nabla I_B(\mathbf{r},\mathbf{\Omega},t)+\beta I_B(\mathbf{r},\mathbf{\Omega},t)=0 \tag{12a}$$

with the boundary condition

$$I_B(\mathbf{r}_w,\mathbf{\Omega},t)=I(\mathbf{r}_w,\mathbf{\Omega},t) \tag{12b}$$

As for the solution of $I_B(\mathbf{r},\mathbf{\Omega},t)$, we consider an approach to equivalently decompose the diffuse irradiation into many collimated beams of different directions, then each collimated irradiation can be solved by Eq. (7) analytically. The diffuse irradiation at the boundary is decomposed into a set of collimated beams of directions $\mathbf{\Omega}_1^c,\mathbf{\Omega}_2^c,\ldots,\mathbf{\Omega}_N^c$, respectively. As a result, the diffuse irradiation is transformed to a set of collimated irradiation problems. This treatment is similar to the modified discrete ordinates method developed by Ramankutty and Crosbie [41] for solving the steady-state radiative transfer problem. Here, the angular discretization and integration of the direct component $I_B(\mathbf{r},\mathbf{\Omega},t)$ takes an approach similar to the discrete ordinates approach. The solid angular space is discretized to N directions. The intensity distribution of the kth collimated irradiation problem $I_B(\mathbf{r},\mathbf{\Omega}_k^c,t)$ is solved by Eq. (7).

By definition, the diffuse component $I_S(\mathbf{r},\mathbf{\Omega},t)$ is governed by

$$\frac{\partial I_S(\mathbf{r},\mathbf{\Omega},t)}{c\partial t}+\mathbf{\Omega}\cdot\nabla I_S(\mathbf{r},\mathbf{\Omega},t)+\beta I_S(\mathbf{r},\mathbf{\Omega},t)=S(\mathbf{r},\mathbf{\Omega},t) \tag{13a}$$

with the boundary condition

$$I_S(\mathbf{r}_w,\mathbf{\Omega},t)=0 \tag{13b}$$

Here, the source function $S(\mathbf{r},\mathbf{\Omega},t)$ is calculated as

$$S(\mathbf{r},\mathbf{\Omega},t)=\kappa_a I_b(\mathbf{r},\mathbf{\Omega},t)+\frac{\kappa_s}{4\pi}\left[\int_{4\pi} I_d(\mathbf{r},\mathbf{\Omega}',t)\Phi(\mathbf{\Omega}',\mathbf{\Omega})\mathrm{d}\Omega'+\sum_{k=1}^{N} I_B\left(\mathbf{r},\mathbf{\Omega}_k^c,t\right)w_k^c\Phi(\mathbf{\Omega}_k^c,\mathbf{\Omega})\right] \tag{14}$$

where w_k^c is the quadrature weight of direction $\mathbf{\Omega}_k^c$. Similarly, the transient incident radiation distribution function $G(\mathbf{r},t)$ and radiative heat flux distribution function $\mathbf{q}(\mathbf{r},t)$ are calculated as

$$G(\mathbf{r},t)=\int_{4\pi} I_S(\mathbf{r},\mathbf{\Omega},t)\mathrm{d}\Omega+\sum_{k=1}^{N} I_B\left(\mathbf{r},\mathbf{\Omega}_k^c,t\right)w_k^c \tag{15a}$$

$$\mathbf{q}(\mathbf{r},t)=\int_{4\pi} I_S(\mathbf{r},\mathbf{\Omega},t)\mathbf{\Omega}\,\mathrm{d}\Omega+\sum_{k=1}^{N} I_B\left(\mathbf{r},\mathbf{\Omega}_k^c,t\right)w_k^c\mathbf{\Omega}_k \tag{15b}$$

III. Discontinuous Spectral Element Discretization

A. Transient Term

Because the transient radiative transfer process often happens in very small time scales (10^{-8} s or less), the discretization of the transient term of Eq. (1) requires a much smaller time step. To avoid numerical overflow, Eq. (1) is transformed to its temporal dimensionless form as

$$\frac{\partial I(\mathbf{r},\mathbf{\Omega},t^*)}{\partial t^*}+L_R\mathbf{\Omega}\cdot\nabla I(\mathbf{r},\mathbf{\Omega},t^*)+L_R\beta I(\mathbf{r},\mathbf{\Omega},t^*)=L_R S(\mathbf{r},\mathbf{\Omega},t^*) \tag{16}$$

where t^* is the dimensionless time defined as $t^*=ct/L_R$, and L_R is a reference length. For the problem of collimated irradiation in a one-dimensional slab, if we choose L_R equal to the width L of the slab, then the value of t^* equals the dimensionless distance that the light beam travels in the slab; for example, when t^*=1, the light beam will travel to a distance L. In some references, the reference length was also given as $L_R=\beta^{-1}$ [12,21,26]. It can be seen that these

definitions are equivalent when $\beta L = 1$. To indicate the wave front of the light beam by the value of t^* for good understanding of the transient radiative transfer process, we take L_R as the characteristic length L of the problem.

The temporal dimensionless TRTE (16) can be written as

$$\frac{\partial I(\mathbf{r}, \mathbf{\Omega}, t^*)}{\partial t^*} = F[I(\mathbf{r}, \mathbf{\Omega}, t^*)] \tag{17}$$

where

$$F[I(\mathbf{r}, \mathbf{\Omega}, t^*)] = -L_R \mathbf{\Omega} \cdot \nabla I(\mathbf{r}, \mathbf{\Omega}, t^*) - L_R \beta I(\mathbf{r}, \mathbf{\Omega}, t^*) + L_R S(\mathbf{r}, \mathbf{\Omega}, t^*) \tag{18}$$

The discretization of the transient term can be written in general form as

$$\frac{I_{t^*+\Delta t^*} - I_{t^*}}{\Delta t^*} = fF[I_{t^*+\Delta t^*}] + (1-f)F[I_{t^*}] \tag{19}$$

where Δt^* is the dimensionless time step and $f \in [0, 1]$ is an adjustment parameter. Taking f as $1/2$, $2/3$, and 1, the Crank–Nicolson, Galerkin, and fully implicit schemes are obtained, respectively. These three schemes are all unconditionally stable, and the Crank–Nicolson scheme has second-order accuracy. Equation (19) can be rewritten as

$$\Omega \cdot \nabla I_n(\mathbf{r}, \mathbf{\Omega}) + \tilde{\beta}_n I_n(\mathbf{r}, \mathbf{\Omega}) = \tilde{S}_n(\mathbf{r}, \mathbf{\Omega}) \qquad n = 1, \ldots, N_t \tag{20}$$

where the subscript n denotes the nth time step, N_t is the total number of time steps, and $\tilde{\beta}_n$ and $\tilde{S}_n(\mathbf{r}, \mathbf{\Omega})$ are defined, respectively, as

$$\tilde{\beta}_n = \frac{1}{L_R \Delta t^* f} + \beta \tag{21}$$

$$\tilde{S}_n(\mathbf{r}, \mathbf{\Omega}) = S_n(\mathbf{r}, \mathbf{\Omega}) + \left(\frac{1}{f} - 1\right) S_{n-1}(\mathbf{r}, \mathbf{\Omega}) - \left(\frac{1}{f} - 1\right) \mathbf{\Omega} \cdot \nabla I_{n-1}(\mathbf{r}, \mathbf{\Omega}) - \left[\beta\left(\frac{1}{f} - 1\right) - \frac{1}{L_R \Delta t^* f}\right] I_{n-1}(\mathbf{r}, \mathbf{\Omega}) \tag{22}$$

It can be seen from Eq. (20) that the temporal discretized TRTE can be written in a form similar to the RTE; thus, a similar approach for solving the RTE can be used to solve Eq. (20).

B. Discontinuous Spectral Element Discretization

Here, the discontinuous spectral element method [38] is applied to solve the discrete ordinates form of Eq. (20). A Chebyshev spectral nodal basis is employed at each element. The radiative intensity field of the nth time step and direction $\mathbf{\Omega}^m$ can be approximated over element K as

$$I_n^m(\mathbf{r}) \simeq \sum_{i=1}^{N_{sk}} I_{n;i}^m \phi_i(\mathbf{r}) \tag{23}$$

where $I_{n;i}^m$ denotes the radiative intensity on the ith node, ϕ_i is the nodal basis of node i, and N_{sk} denotes the number of solution nodes on K. For each element K, the discrete ordinates form of Eq. (20) is weighted by ϕ_j and integrated over K using Gauss divergence theorem. This leads to

$$-\int_K I_n^m \mathbf{\Omega}^m \cdot \nabla \phi_j \, \mathrm{d}V + \int_{\partial K} \widehat{\mathbf{\Omega}^m I_n^m} \cdot \mathbf{n}_{\partial K} \phi_j \, \mathrm{d}A + \int_K \tilde{\beta}_n I_n^m \phi_j \, \mathrm{d}V = \int_K \tilde{S}_n^m \phi_j \, \mathrm{d}V \tag{24}$$

where superscript m denotes the discrete ordinates direction, and $\mathbf{n}_{\partial K}$ denotes the unit normal vector of the boundary of element K. The numerical flux $\widehat{\mathbf{\Omega}^m I_n^m}$ is modeled by the local Lax–Friedrichs scheme as

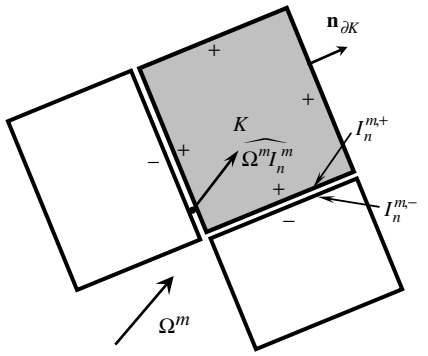

Fig. 2 Schematic of the variables defined in the discontinuous spectral element method.

$$\widehat{\mathbf{\Omega}^m I_n^m} = \mathbf{\Omega}^m \left\{ I_n^m \right\} + |\mathbf{\Omega}^m| \left[\left[I_n^m \right]\right] \mathbf{n}_{\partial K} \tag{25}$$

Here, the operators $\{\cdot\}$ and $[[\cdot]]$ denote the mean value and the jump value of arguments across the interelement boundary:

$$\left\{ I_n^m \right\} = \tfrac{1}{2}\left(I_n^{m,+} + I_n^{m,-} \right), \qquad \left[\left[I_n^m \right]\right] = \tfrac{1}{2}\left(I_n^{m,+} - I_n^{m,-} \right) \tag{26}$$

where the superscript operators $+$ and $-$ denote the values at the boundary inside element K and outside element K, respectively, which are defined, respectively, as

$$I_n^{m,+} = \lim_{\delta \to 0} I_n^m(\mathbf{r}_{\partial K} - \delta \mathbf{n}_{\partial K}), \qquad I_n^{m,-} = \lim_{\delta \to 0} I_n^m(\mathbf{r}_{\partial K} + \delta \mathbf{n}_{\partial K}) \tag{27}$$

Figure 2 shows the relation of variables defined in the discontinuous spectral element method for good understanding. By substituting Eqs. (23) and (25) into Eq. (24), the final discretization over element K can be simply written as

$$\mathbf{M}_n^m \mathbf{I}_n^m = \mathbf{H}_n^m \tag{28}$$

where the matrices $\mathbf{M}_n^m$ and $\mathbf{H}_n^m$ are defined, respectively, as

$$M_{n;ji}^m = -\int_K \phi_i \Omega^m \cdot \nabla \phi_j \, \mathrm{d}V + \frac{1}{2}\int_{\partial K} (\Omega^m \cdot \mathbf{n}_{\partial K} + |\Omega^m|) \phi_i \phi_j \, \mathrm{d}A + \int_K \tilde{\beta}_n \phi_i \phi_j \, \mathrm{d}V \tag{29a}$$

$$H_{n;j}^m = \int_K \tilde{S}_n^m \phi_j \, \mathrm{d}V - \frac{1}{2}\int_{\partial K} (\mathbf{\Omega}^m \cdot \mathbf{n}_{\partial K} - |\mathbf{\Omega}^m|) I_n^{m,-} \phi_j \, \mathrm{d}A \tag{29b}$$

C. Solution Procedures

As shown in Eq. (20), the solution of the TRTE requires the solution of a RTE-like equation at each time step. At each time step, Eq. (20) is solved element by element. On each element, the matrix equations given by Eq. (28) are solved by Gaussian elimination. The implementation of this discontinuous spectral element method can be carried out according to the following routine:

1) Decompose the solution domain with nonoverlap elements and generate spectral nodes on each element according to the polynomial order p.

2) Initialize the radiative intensity field.

3) Loop at each time step, $n = 1, \ldots, N_t$.

4) If collimated irradiation is considered, then calculate the collimated component $I_c(\mathbf{r}, \mathbf{\Omega}, n\Delta t^*)$ according to Eq. (7).

5) Calculate matrices $\mathbf{M}_n^m$ and $\mathbf{H}_n^m$ and solve matrix equation Eq. (28) element by element to solve Eq. (20) in each direction. As for the collimated irradiation problem, solve $I_d(\mathbf{r}, \mathbf{\Omega}, n\Delta t^*)$, else for diffuse irradiation, solve $I_S(\mathbf{r}, \mathbf{\Omega}, n\Delta t^*)$. For the other case, directly solve the radiative intensity field $I(\mathbf{r}, \mathbf{\Omega}, n\Delta t^*)$.

6) If the time loop does not finish, go to step 3, else do postprocessing.

The maximum relative error 10^{-4} of incident radiation $\|G_{\text{new}} - G_{\text{old}}\|/\|G_{\text{new}}\|$ is given as the stop criterion for the solution of Eq. (20) at each time step.

IV. Results and Discussion

Three test cases are selected to check the performances of the DSEM for solving transient radiative transfer in semitransparent media. The Crank–Nicolson scheme is given as temporal discretization for all following computation. For the sake of quantitative comparison with the benchmark results, the integration averaged relative error of the DSEM solution is defined as

$$\text{relative error } \% = \frac{\int |\text{DSEM solution} - \text{benchmark result}|\,\mathrm{d}x}{\int |\text{benchmark result}|\,\mathrm{d}x} \times 100 \tag{30}$$

A. Case 1: Collimated Irradiation Inside an Infinite Slab

We consider one-dimensional transient radiative transfer in an infinite slab. The media is absorbing and isotropically scattering with scattering albedo of $\omega = 0.5$. The optical thickness based on width L of the slab is $\tau_L = \beta L = 1$. The left boundary ($x/L = 0$) and the right boundary ($x/L = 1$) are black and both the boundaries and the media are kept cold. Initially ($t = 0$), a collimated beam of unit intensity is suddenly irradiated normal to the left boundary and then held constant. The DSEM was applied to solve the incident radiation and radiative heat flux distribution inside the slab. Figures 3a and 3b show the incident radiation and heat flux distribution at different dimensionless times, respectively, and are compared with the results obtained by the IE method [17]. In this study, the slab is equally subdivided into 10 elements, with second-order polynomial approximation used on each element, and the angular space is discretized by S_8 approximation. The dimensionless time step is given as $\Delta t^* = 0.02$. The result obtained by the IE method [17] uses

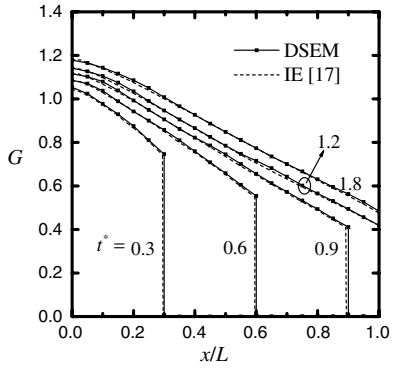

a)

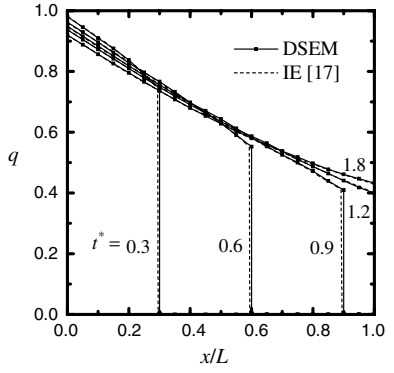

b)

Fig. 3 Solutions obtained by the DSEM: a) incident radiation and b) heat flux distribution at different dimensionless times.

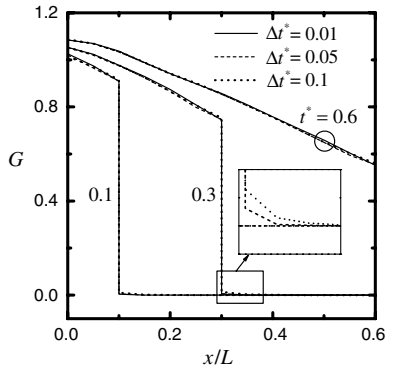

Fig. 4 Incident radiation distribution of different times obtained with different time steps.

100 spatial elements with a dimensionless time step of $\Delta t^* = 0.01$. By comparison, the results of the DSEM agree with those of the IE method very well. The DSEM shows better performance in capturing the discontinuous wave front.

To study the influence of temporal discretization on the DSEM result, Fig. 4 shows the incident radiation distribution of different times obtained by the DSEM with three different time steps: $\Delta t^* = 0.01, 0.05$, and 0.1, respectively. With the increase of the time step, the accuracy of temporal integration decreases, which results in an increasing of numerical diffusion.

Because of the particularity of the discontinuous Galerkin scheme (it only allows discontinuity existing at the element boundary and still uses continuous approximation inside each element), the accuracy of capturing the wave front is dependent on and limited to the size of the element and the time step. To further study the performance of the DSEM when a discontinuous wave front does not coincide with the element boundary, Figs. 5a and 5b show the incident radiation distribution and heat flux distribution of different times, respectively. Here, the slab is subdivided into five elements

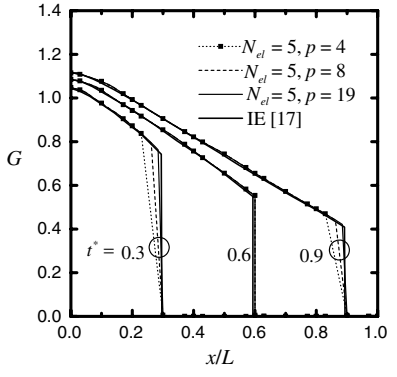

a)

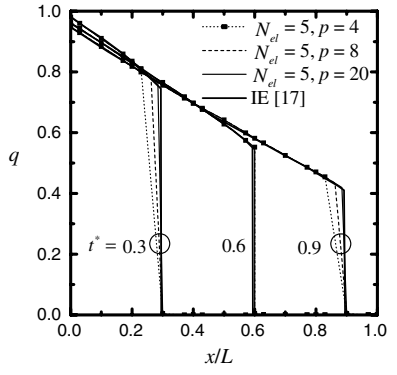

b)

Fig. 5 Influence of coincidence of the wave front with the element boundary and polynomial order on the DSEM: a) incident radiation and b) heat flux distribution at different dimensionless times.

with various polynomial orders ($p = 4$, 8, and 20), and the time step is given as $\Delta t^* = 0.02$. It can be seen that the wave front is not well-captured when $t^* = 0.3$ and 0.9 (when the wave front does not coincide with the element boundary). However, the discontinuous wave front can be effectively captured with increasing polynomial order, in case it does not coincide with the element boundary.

B. Case 2: Diffuse Irradiation Inside a One-Dimensional Slab

In this case, the configuration and specification of the properties of the media and boundaries are the same as in the previous case. Initially ($t = 0$), the temperature of the left boundary is suddenly increased to provide a unit radiative power and then held constant. This case has been studied by several researchers [17,27,44] and serves as a good test case to verify the performance of the numerical method for transient radiative transfer. The DSEM was applied to solve the incident radiation and radiative heat flux distribution inside the slab. Special treatment for diffuse irradiation is used: the diffuse irradiation is equivalently decomposed to many collimated irradiation. In the following analysis, the dimensionless time step of $\Delta t^* = 0.01$ is given for all the computation in this section.

Figures 6a and 6b show the incident radiation and heat flux distribution at different dimensionless times, respectively, compared with the results obtained by the IE method [17]. The slab is uniformly subdivided into 10 elements with fourth-order polynomial approximation. The diffuse irradiation on the left boundary is decomposed into $N_\theta^c = 200$ directions of collimated beam; these directions are determined by the piecewise constants angular (PCA) scheme and used for the angular integration used in Eq. (15). Angular discretization for solving the diffuse component takes PCA approximation with $N_\theta = 20$. As shown in Fig. 6, the DSEM can accurately capture the wave front: the results of the DSEM agree with those of the IE method [17] very well. Figures 7a and 7b show the incident radiation and heat flux distribution at different dimensionless times in which second-order polynomial approximation for spatial discretization and different angular discretization schemes are used. Even with very rough angular discretization such as S_4 approximation, the results of the DSEM agree with those of the IE method very well. The influence of the number of equivalent beams N_θ^c on the performance of the DSEM is shown in Fig. 8. When N_θ^c is small, there are nonphysical oscillations in the solved incident radiation by the DSEM, but with the increasing of N_θ^c, the oscillations are effectively mitigated.

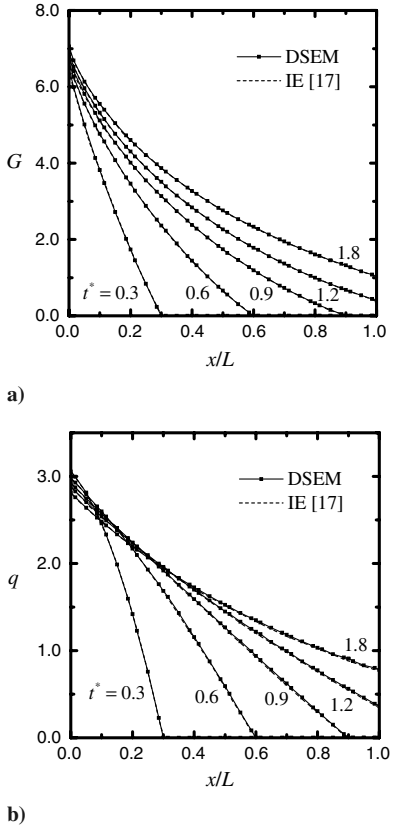

Fig. 6 Solutions obtained by the DSEM: a) incident radiation and b) heat flux distribution at different dimensionless times.

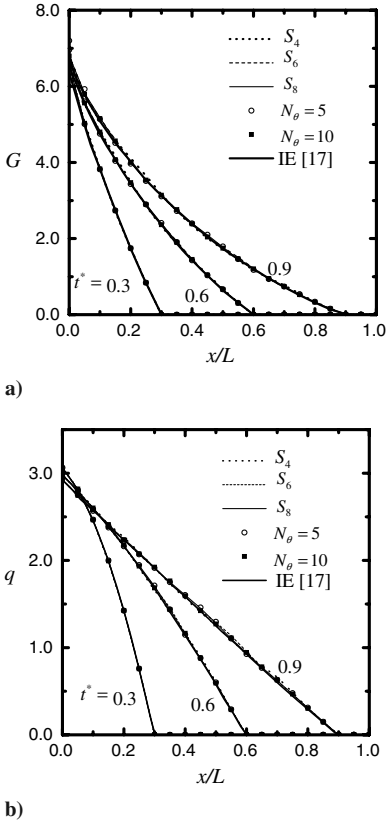

Fig. 7 Angular refinement study for the DSEM with special treatment for diffuse irradiation: a) the incident radiation and b) heat flux distribution at different dimensionless times.

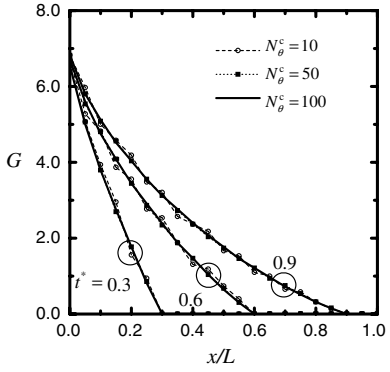

Fig. 8 Influence of the number of equivalent beams $N_{\theta'}$ on the performance of the DSEM.

A comparison of the DSEM solution with and without special treatment for diffuse irradiation is presented in Fig. 9, in which the incident radiation distribution at different dimensionless times is obtained by the present approach, and is compared with the results of the IE method [17]. Here, the solutions obtained based on the general governing equation (without special treatment for diffuse irradiation) are denoted as GDSEM. Second-order approximation is used on each element. It can be seen that the results of the GDSEM are obvious nonphysical oscillations when the angular discretization is rough ($N_\theta = 20$), whereas with angular refinement ($N_\theta = 40$), these nonphysical oscillations can be mitigated to a large extent, which is attributed to ray effect. However, the results of the DSEM are much better than those of the GDSEM under the same spatial and angular

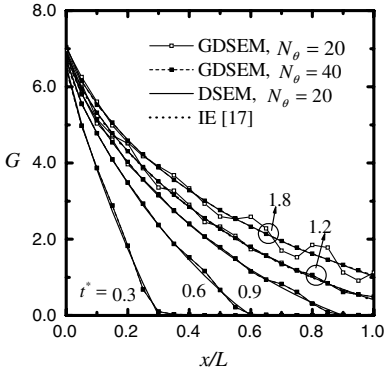

Fig. 9 Comparison of the DSEM solution with and without special treatment for diffuse irradiation.

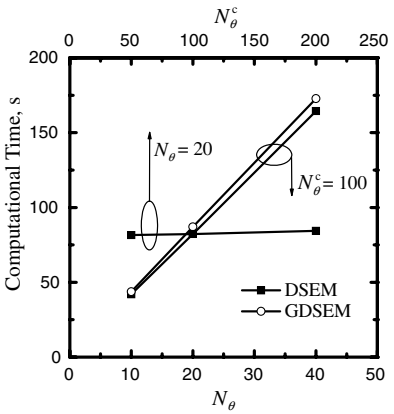

Fig. 10 Comparison of computational times of the GDSEM and DSEM.

discretization compared with the benchmark results obtained using the IE method [17].

To check the efficiency of the DSEM with special treatment, Fig. 10 shows the computational time of both schemes under the same spatial discretization ($N_{\text{el}} = 10$ and $p = 2$) and different angular discretization when dimensionless times are increased to $t^* = 1.8$. With the increasing of angular discretization (PCA discretization with N_θ increase from 10 to 40), both the computational time of the DSEM and the GDSEM are linearly increasing. This was because the computational effort of discrete ordinates solution process is proportional to angular discretization. For the DSEM, it requires the solution of two subproblems: the equivalent collimated irradiation problem and the solution of the discrete ordinates equation (13). As a result, the number of beams given in the special treatment (N_θ^c) will influence the total computational time. This study shows that with the increasing of N_θ^c from 50 to 200, the total computational time increases little. This is attributed to the analytical solution process of the equivalent collimated irradiation being very efficient. Generally, the DSEM is very efficient.

C. Case 3: Two-Dimensional Irregular Configuration

In this case, the DSEM is applied to transient radiative transfer in a two-dimensional irregular enclosure. The configuration of the enclosure is shown in Fig. 11a. The media is absorbing and emitting with absorption coefficient of $\kappa_a = 1\ \text{m}^{-1}$. All the boundaries are black. Initially, the temperature of the media and boundary are 0 K. At $t^* = 0$, the media temperature was suddenly increased to T_g and maintained. Three spatial discretization schemes are used to check the performance of the DSEM: 1) 16 regular elements, 2) 16 irregular elements, and 3) 64 regular elements, which are shown in Fig. 11. In this study, the time step is given as $\Delta t^* = 0.01$, fourth-order polynomial approximation is used on each element, and angular discretization takes S_8 approximation.

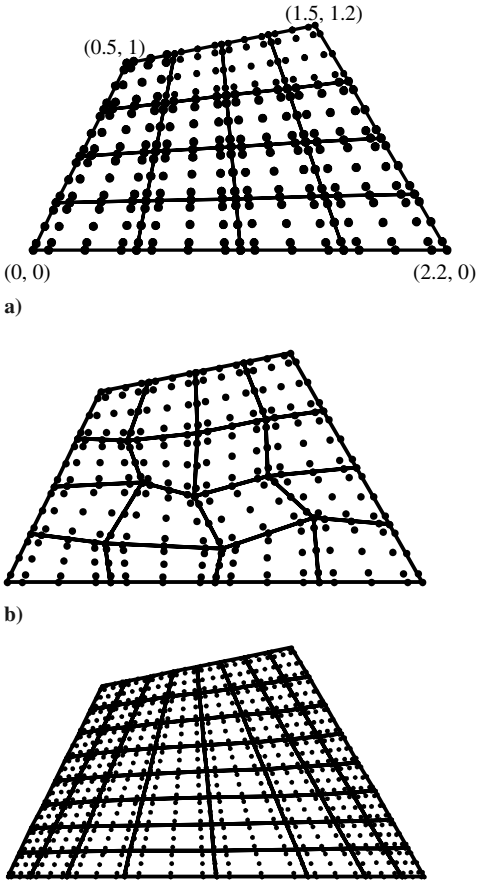

Fig. 11 Configuration of the irregular quadrilateral enclosure and mesh decomposition and spectral node distribution ($p = 4$): a) 16 elements, b) irregular 16 elements, and c) 64 elements.

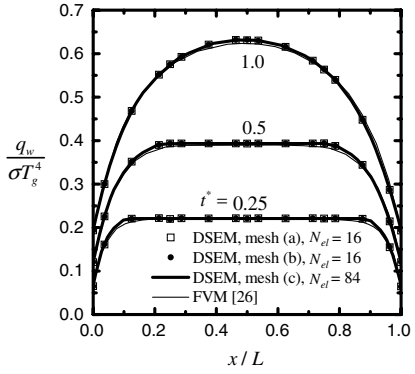

Fig. 12 Dimensionless radiative heat flux distributions along the bottom wall of the irregular quadrilateral enclosure at different dimensionless times.

Figure 12 shows the dimensionless radiative heat flux along the bottom wall of different times obtained by the DSEM with three spatial decomposition schemes shown in Figs. 11a–11c and compared with the results obtained by the FVM [26]. The results of the DSEM agree with those of the FVM [26] very well, even in the case of skewed mesh and far fewer elements. The maximum integral averaged error based on the result of the FVM [26] is less than 2%. Generally, the DSEM is effective for solving multidimensional transient radiative transfer problems.

V. Conclusions

A discontinuous spectral element method is presented to solve transient radiative heat transfer in multidimensional semitransparent media. The transient term is discretized by the Crank–Nicolson

scheme, and the spatial discretization is conducted by the discontinuous spectral element approach. The DSEM is of high-order accuracy and has properties such as local conservation, and solutions are allowed to be discontinuous across interelement boundaries. The DSEM is demonstrated to be able to efficiently and accurately capture the sharp wave front of the transient radiative transfer process. A special treatment for the diffuse irradiation boundary is presented to mitigate the ray effect encountered in general treatment. The predicted results by the DSEM agree well with reported benchmark solutions in the references. The DSEM with special treatment for diffuse irradiation effectively mitigates the ray effect and gives very accurate results. Because of the high accuracy of spatial discretization, accurate result can be obtained by the DSEM even with a relatively small number of elements.

Acknowledgment

The support of this work by the National Nature Science Foundation of China (grants 50636010 and 50425619) is gratefully acknowledged.

References

[1] Qui, T. G., and Tien, C. L., "Short Pulse Laser Heating in Metals," *International Journal of Heat and Mass Transfer*, Vol. 35, No. 3, 1992, pp. 719–726. doi:10.1016/0017-9310(92)90131-B

[2] Longtin, J. P., and Tien, C. L., "Saturable Absorption During High-Intensity Laser Heating of Liquids," *Journal of Heat Transfer*, Vol. 118, No. 4, 1996, pp. 924–930.

[3] Kumar, S., and Mitra, K., "Microscale Aspects of Thermal Radiation Transport and Laser Applications," *Advances in Heat Transfer*, Vol. 33, Feb. 1999, pp. 187–294.

[4] Yamada, Y., "Light-Tissue Interaction and Optical Imaging in Biomedicine," *Annual Review of Heat Transfer*, Vol. 6, No. 6, 1995, pp. 1–59.

[5] Popp, A. K., Valentine, M. T., Kaplan, P. D., and Weitz, D. A., "Microscopic Origin of Light Scattering in Tissue," *Applied Optics*, Vol. 42, No. 16, 2003, pp. 2871–2880. doi:10.1364/AO.42.002871

[6] Patterson, M. S., Wilson, B. C., and Wyman, D. R., "The Propagation of Optical Radiation in Tissue, 1: Models of Radiation Transport and Their Application," *Lasers in Medical Science*, Vol. 6, No. 2, 1991, pp. 155–168. doi:10.1007/BF02032543

[7] Okada, E., Firbank, M., Schweiger, M., Arridge, S. R., Cope, M., and Delpy, D. T., "Theoretical and Experimental Investigation of Near-Infrared Light Propagation in a Model of the Adult Head," *Applied Optics*, Vol. 36, No. 1, 1997, pp. 21–31.

[8] Nussbaum, E. L., Baxter, G. D., and Lilge, L., "A Review of Laser Technology and Light-Tissue Interactions as a Background to Therapeutic Applications of Low Intensity Lasers and Other Light Sources," *The Physical Therapy Review*, Vol. 8, No. 1, 2003, pp. 31–44. doi:10.1179/108331903225001381

[9] Hebden, J. C., Veenstra, H., Dehghani, H., Hillman, E. M. C., Schweiger, M., Arridge, S. R., and Delpy, D. T., "Three-Dimensional Time-Resolved Optical Tomography of a Conical Breast Phantom," *Applied Optics*, Vol. 40, No. 19, 2001, pp. 3278–3287. doi:10.1364/AO.40.003278

[10] Arridge, S. R., "Optical Tomography in Medical Imaging," *Inverse Problems*, Vol. 15, No. 2, 1999, pp. R41–R93. doi:10.1088/0266-5611/15/2/022

[11] Fercher, A. F., Drexler, W., Hitzenberger, C. K., and Lasser, T., "Optical Coherence Tomography—Principles and Applications," *Reports on Progress in Physics*, Vol. 66, No. 2, 2003, pp. 239–303. doi:10.1088/0034-4885/66/2/204

[12] Sakami, M., Mitra, K., and Vo-Dinh, T., "Analysis of Short-Pulse Laser Photon Transport Through Tissues for Optical Tomography," *Optics Letters*, Vol. 27, No. 5, 2002, pp. 336–338. doi:10.1364/OL.27.000336

[13] Guo, Z., Kumar, S., and San, K., "Multidimensional Monte Carlo Simulation of Short-Pulse Laser Transport in Scattering Media," *Journal of Thermophysics and Heat Transfer*, Vol. 14, No. 4, 2000, pp. 504–511.

[14] Hsu, P.-f., "Effects of Multiple Scattering and Reflective Boundary on the Transient Radiative Transfer Process," *International Journal of Thermal Sciences*, Vol. 40, No. 6, 2001, pp. 539–549. doi:10.1016/S1290-0729(01)01242-X

[15] Gentile, N. A., "Implicit Monte Carlo Diffusion: An Acceleration Method for Monte Carlo Time-Dependent Radiative Transfer Simulations," *Journal of Computational Physics*, Vol. 172, No. 2, 2001, pp. 543–571. doi:10.1006/jcph.2001.6836

[16] Sakami, M., Mitra, K., and Hsu, P. F., "Analysis of Light-Pulse Transport Through Two-Dimensional Scattering and Absorbing Media," *Journal of Quantitative Spectroscopy and Radiative Transfer*, Vol. 73, Nos. 2–5, 2002, pp. 169–179. doi:10.1016/S0022-4073(01)00216-3

[17] Tan, Z. M., and Hsu, P. F., "An Integral Formulation of Transient Radiative Transfer," *Journal of Heat Transfer*, Vol. 123, No. 3, 2001, pp. 466–475. doi:10.1115/1.1371230

[18] Wu, C. Y., "Propagation of Scattered Radiation in a Participating Planar Medium with Pulse Irradiation," *Journal of Quantitative Spectroscopy and Radiative Transfer*, Vol. 64, No. 5, 2000, pp. 537–548. doi:10.1016/S0022-4073(99)00151-X

[19] Wu, C. Y., and Wu, S. H., "Integral Equation Formulation for Transient Radiative Transfer in an Anisotropically Scattering Medium," *International Journal of Heat and Mass Transfer*, Vol. 43, No. 11, 2000, pp. 2009–2020. doi:10.1016/S0017-9310(99)00262-8

[20] Mitra, K., and Kumar, S., "Development and Comparison of Models for Light-Pulse Transport Through Scattering-Absorbing Media," *Applied Optics*, Vol. 38, No. 1, 1999, pp. 188–196.

[21] Guo, Z., and Kumar, S., "Discrete-Ordinates Solution of Short-Pulsed Laser Transport in Two-Dimensional Turbid Media," *Applied Optics*, Vol. 40, No. 19, 2001, pp. 3156–3163. doi:10.1364/AO.40.003156

[22] Guo, Z., and Kumar, S., "Three-Dimensional Discrete Ordinates Method in Transient Radiative Transfer," *Journal of Thermophysics and Heat Transfer*, Vol. 16, No. 3, 2002, pp. 289–296.

[23] Guo, Z., and Kim, K. H., "Ultrafast-Laser-Radiation Transfer in Heterogeneous Tissues with the Discrete-Ordinates Method," *Applied Optics*, Vol. 42, No. 16, 2003, pp. 2897–2905. doi:10.1364/AO.42.002897

[24] Mitra, K., Lai, M.-S., and Kumar, S., "Transient Radiation Transport in Participating Media with a Rectangular Enclosure," *Journal of Thermophysics and Heat Transfer*, Vol. 11, No. 3, 1997, pp. 409–414.

[25] Chai, J. C., "One-Dimensional Transient Radiation Heat Transfer Modeling Using a Finite-Volume Method," *Numerical Heat Transfer, Part B, Fundamentals*, Vol. 44, No. 2, 2003, pp. 187–208. doi:10.1080/713836346

[26] Chai, J. C., "Transient Radiative Transfer in Irregular Two-Dimensional Geometries," *Journal of Quantitative Spectroscopy and Radiative Transfer*, Vol. 84, No. 3, 2004, pp. 281–294. doi:10.1016/S0022-4073(03)00183-3

[27] An, W., Ruan, L. M., Tan, H. P., and Qi, H., "Least-Squares Finite Element Analysis for Transient Radiative Transfer in Absorbing and Scattering Media," *Journal of Heat Transfer*, Vol. 128, No. 5, 2006, pp. 499–503. doi:10.1115/1.2190694

[28] Liu, L. H., and Hsu, P.-F., "Analysis of Transient Radiative Transfer in Semitransparent Graded Index Medium," *Journal of Quantitative Spectroscopy and Radiative Transfer*, Vol. 105, No. 3, 2007, pp. 357–376. doi:10.1016/j.jqsrt.2006.12.003

[29] Cui, X., and Li, B. Q., "Discontinuous Finite Element Solution of 2-D Radiative Transfer with and without Axisymmetry," *Journal of Quantitative Spectroscopy and Radiative Transfer*, Vol. 96, Nos. 3–4, 2005, pp. 383–407. doi:10.1016/j.jqsrt.2004.11.007

[30] Cui, X., and Li, B. Q., "A Discontinuous Finite-Element Formulation for Internal Radiation Problems," *Numerical Heat Transfer, Part B, Fundamentals*, Vol. 46, No. 3, 2004, pp. 223–242. doi:10.1080/10407790490475274

[31] Bassi, F., and Rebay, S., "High-Order Accurate Discontinuous Finite Element Solution of the 2D Euler Equations," *Journal of Computational Physics*, Vol. 138, No. 2, 1997, pp. 251–285. doi:10.1006/jcph.1997.5454

[32] Cockburn, B., and Shu, C. W., "The Runge-Kutta Discontinuous Galerkin Method for Conservation Laws V: Multidimensional Systems," *Journal of Computational Physics*, Vol. 141, No. 2, 1998, pp. 199–224. doi:10.1006/jcph.1998.5892

[33] Baumann, C. E., and Oden, J. T., "A Discontinuous HP Finite Element Method for Convection-Diffusion Problems," *Computer Methods in Applied Mechanics and Engineering*, Vol. 175, No. 3, 1999, pp. 311–341.
doi:10.1016/S0045-7825(98)00359-4

[34] Warburton, T. C., and Karniadakis, G. E., "A Discontinuous Galerkin Method for the Viscous MHD Equations," *Journal of Computational Physics*, Vol. 152, No. 2, 1999, pp. 608–641.
doi:10.1006/jcph.1999.6248

[35] Cockburn, B., "Discontinuous Galerkin Methods," *ZAMM*, Vol. 83, No. 11, 2003, pp. 731–754.
doi:10.1002/zamm.200310088

[36] Cockburn, B., Karniadakis, G. E., and Shu, C. W., *The Development of Discontinuous Galerkin Methods*, Springer Verlag, Berlin, 2000, pp. 3–50.

[37] Karniadakis, G. E., and Sherwin, S. J., *Spectral/HP Element Methods for CFD*, Oxford Univ. Press, New York, 1999.

[38] Zhao, J. M., and Liu, L. H., "Discontinuous Spectral Element Method for Solving Radiative Heat Transfer in Multidimensional Semi-transparent Media," *Journal of Quantitative Spectroscopy and Radiative Transfer*, Vol. 107, No. 1, 2007, pp. 1–16.
doi:10.1016/j.jqsrt.2007.02.001

[39] Zhao, J. M., and Liu, L. H., "Least-Squares Spectral Element Method for Radiative Heat Transfer in Semitransparent Media," *Numerical Heat Transfer, Part B, Fundamentals*, Vol. 50, No. 5, 2006, pp. 473–489.
doi:10.1080/10407790600682821

[40] Modest, M. F., *Radiative Heat Transfer*, McGraw–Hill, New York, 1993.

[41] Ramankutty, M. A., and Crosbie, A. L., "Modified Discrete Ordinates Solution of Radiative Transfer in Two-Dimensional Rectangular Enclosures," *Journal of Quantitative Spectroscopy and Radiative Transfer*, Vol. 57, No. 1, 1997, pp. 107–140.
doi:10.1016/S0022-4073(96)00090-8

[42] Olfe, D. B., "A Modification of the Differential Approximation for Radiative Transfer," *AIAA Journal*, Vol. 5, No. 4, 1967, pp. 638–643.

[43] Modest, M. F., "Modified Differential Approximation for Radiative Transfer in General Three- Dimensional Media," *Journal of Thermophysics and Heat Transfer*, Vol. 3, No. 3, 1989, pp. 283–288.

[44] Katika, K. M., and Pilon, L., "Modified Method of Characteristics in Transient Radiation Transfer," *Journal of Quantitative Spectroscopy and Radiative Transfer*, Vol. 98, No. 2, 2006, pp. 220–237.
doi:10.1016/j.jqsrt.2005.05.086